

# Variations in CO, O<sub>3</sub> and black carbon aerosol mass concentrations associated with planetary boundary layer (PBL) over tropical urban environment in India

K. V. S. Badarinath · Anu Rani Sharma ·  
Shailesh Kumar Kharol · V. Krishna Prasad

Received: 3 April 2009 / Accepted: 15 September 2009 /  
Published online: 29 September 2009  
© Springer Science + Business Media B.V. 2009

**Abstract** Carbon monoxide (CO), Ozone (O<sub>3</sub>) and Black Carbon (BC) aerosol mass concentrations in relation to planetary boundary layer (PBL) height measurements were analyzed from January–December, 2008 over tropical urban environment of Hyderabad, India. DMSP-OLS night-time satellite data were analyzed for fire occurrence over the region and its correlation with pollution concentrations over the urban region. Results of the study suggested considerable increase in CO and BC concentrations during early morning hours. Higher concentration of BC, CO and ozone was observed during pre-monsoon, post-monsoon and winter and lowest concentrations exhibited during monsoon season. NCEP/NCAR reanalysis winds suggested long range transport of aerosols and trace gases from forest fires are enhancing the pollutant concentrations over the study area.

**Keywords** Planetary boundary layer (PBL) · BC · CO · Ozone and forest fires

## 1 Introduction

Rapid population growth together with industrialization and exponential growth in vehicular fleet are contributing to deteriorating air quality in several urban regions of India (Jain and Khare 2008). Nearly 25% of the total energy (of which 98% comes from oil) in India is consumed by transport sector contributing more than 50–80% of air pollution

---

K. V. S. Badarinath (✉) · A. R. Sharma · S. K. Kharol  
Atmospheric Science Section, National Remote Sensing Centre, Dept. of Space-Govt. of India,  
Balanagar, Hyderabad 500 625, India  
e-mail: badrinath\_kvs@nrsc.gov.in

A. R. Sharma  
e-mail: bhardwaj\_anu2003@yahoo.co.in

S. K. Kharol  
e-mail: shaileshan2000@yahoo.co.in

V. K. Prasad  
Agroecosystem Management Program, The Ohio State University, Columbus, OH, USA  
e-mail: krisvbkp@yahoo.com

problem in most of the metro cities (Molina and Molina 2004). The most important primary pollutants include carbon monoxide (CO), oxides of nitrogen (NO, NO<sub>x</sub>), sulphur oxides (SO<sub>x</sub>), soot, dust and non-methane hydrocarbons (NMHC), in particular benzene, toluene and xylene. In addition, secondary trace gases which can be formed from these precursor substances in certain photochemical reaction conditions include nitrogen dioxide (NO<sub>2</sub>), ozone (O<sub>3</sub>) and other photo-oxidants, e.g., peroxyacetyl nitrate (PAN) (Logan et al. 1981). Vehicles in major metropolitan cities are estimated to account for 70% of CO, 50% of HC, 30–40% of NO<sub>x</sub>, 30% of SPM and 10% of SO<sub>2</sub> of the total pollution loads, of which about two third is contributed by two wheelers alone (Goyal et al. 2006). The adverse effects from these pollutants have both short-term and long-term health impacts.

Although, most of the atmospheric composition in the urban areas is largely influenced by traffic induced pollutants, several other indirect sources enhance the pollutant levels. Hyderabad (17°10' and 17°50'N and 78°10' and 78°50' E) is the fifth largest city in India with a population according to 2001 census is 5,751,780. The climate of the region is semi-arid and the area experiences four dominant seasons each year: winter (January–February), pre-monsoon (March–May), monsoon (June–September) and post monsoon (October–December). In particular, during the pre-monsoon season, due to frequent dust storms and dry spells of weather, the air masses carry dry dust particles from the western Thar Desert to the study region (Badarinath et al. 2007c, d). Also, the other pollutant sources include combustion processes (e.g., including the burning of fossil fuels for steam and power generation, heating and household cooking, waste burning and gasoline and diesel-fueled engine combustion) and other non-combustion industrial processes (e.g., solvent extraction), etc. Most importantly, biomass burning from slash and burn agriculture crop practices, locally called “Jhum cultivation” are one of the major causes of increased pollutant levels during pre-monsoon season. Biomass burning is a significant source of atmospheric trace gases and aerosol particles which affect the atmospheric chemistry and the radiation budget on a global scale by contributing significant amount of aerosol and trace gases to the troposphere (Andreae and Merlet 2001; Badarinath et al. 2006). Also, the dispersion of pollutants is dependent upon many meteorological parameters (Collier et al. 2005), most significant being wind speed and boundary layer depth that defines the volume of air through which the pollution is mixed.

The present study address the following questions: (1) How does CO, O<sub>3</sub> and BC mass concentration vary during January–December, 2008 in the study area (2) How does nighttime planetary boundary layer height and local meteorology influence these variations (3) Which other ancillary sources influence pollutant concentrations during the pre-monsoon season?. We have used intense ground based measurements of CO, O<sub>3</sub> and black carbon in addition to nocturnal planetary boundary layer (PBL) measurements from LIDAR to address these questions. DMSP-OLS night-time satellite data were analyzed to quantify forest fires over the region and their influence on the pollutant levels over urban region of Hyderabad. National Center for Environmental Prediction (NCEP) winds and local weather station data were analyzed to address the long range transport of pollutants over the region.

## 2 Data

### 2.1 Pollutant and meteorological data

Continuous and near-real-time measurements of the black carbon (BC) aerosol mass concentration were carried out using an Aethalometer; model AE-21 of Magee Scientific, USA (Cooke et al. 1997; Latha and Badarinath 2003a, b) during January–December, 2008.

Aethalometer aspirates ambient air from an altitude of 3 m above the ground using its inlet tube and its pump. The BC mass concentration was estimated by measuring the change in the transmittance of a quartz filter tape, on to which the particles impinge. The instrument was operated continuously at a flow rate of 3LPM using a 5-min integration time. The instrument performs diagnostic checks and provides an estimate of its internal noise and BC resolution. The instrument has been factory calibrated at periodical intervals and errors in measurements are  $\pm 2\%$  (Badarinath et al. 2007a).

In addition to BC, synchronous measurements of surface ozone were carried out using  $O_3$  analyser (41M of Environment S.A, France) based on UV absorption radiation at 253.7 nm by ozone molecules. The analyser incorporates corrections due to changes in temperature, pressure in the absorption cell and drift in the intensity of the UV lamp. Carbon monoxide (CO) was measured using CO11M analyser (Environment S. A.) by IR absorption at 4.67  $\mu\text{m}$ . CO calibration has been carried out using reference gas samples. The details on these analyzers are described in the literature (Naja and Lal 2002; Nair et al. 2002; Reddy et al. 2008). The meteorological data during January–December, 2008 were collected from the METOS weather station installed at the measurement site. Wind speed and direction at 925 mb from National Center for Environmental Prediction (NCEP) were analyzed for the period of January–December, 2008.

## 2.2 Planetary boundary layer (PBL) measurements

In the present study, nocturnal PBL height measurements were carried out during the period of January–December, 2008 using Portable Micro pulse Lidar system fabricated by National Atmospheric Research Laboratory (NARL) (Kumar 2006). The LIDAR system was operating under cloudless conditions from evening 06:00 PM (1800 h local time) to morning 06:00 AM (0600 h local time). The system employs a diode pumped Nd: YAG laser with second harmonic output at 532 nm and operated at 2,500 Hz repetition rate and 10  $\mu\text{J}$  output pulse energy. The emitter beam is coaxial to receiver field of view (FOV) and operated in zenith direction. The lidar receiver employs a 150-mm Cassegrain telescope and a high gain photo multiplier tube (PMT) operating in photon counting mode. The complete overlap between the laser beam and the telescope FOV is expected at 150 m. This value represents the lower limit of our vertical lidar profile. The backscattered signals are measured with a bin width of 200 ns corresponding to the altitude range of 30 m. Computer based multi-channel analyser (MCA) was employed for recording the photon returns. The raw data profile was integrated every 2 min interval and this correspond to 3 lakh shots integrated photon-count profile. The lidar measures height profile of backscattered signal from aerosols, during clear-sky, which are converted into backscattering ratio (R). The aerosol backscattering ratio, R is defined as,

$$R = \frac{(\beta_a + \beta_m)}{\beta_m} \quad (1)$$

Where  $\beta_a$  and  $\beta_m$  are the backscatter coefficients of aerosol and molecules, respectively. The aerosol backscatter ratio from the lidar return was estimated using the inversion method suggested in the literature (Klett 1981). The extinction coefficient 'k' and optical thickness ( $\tau_{532}$ ) were estimated from lidar data using,

$$k = S_a * \beta_a, \quad (2)$$

$$\tau_{532} = \int k(z) dz, \quad (3)$$

Where  $z$  is the range between the laser source and the target ( $\sim 7$  km).  $S_d$  is lidar ratio or extinction to backscattering ratio taken as 50 sr. PBL height was calculated from the second-derivative profile of BSR ratio (Chen et al. 2001).

### 2.3 Spatial analysis of fires using DMSP-OLS data

DMSP-OLS data for the year 2008 provided via an automated subscription service from the NOAA National Geophysical Data Center (NGDC) in Boulder, Colorado, USA, were processed for active forest fire locations over entire Indian region, including Hyderabad and its environs (Elvidge et al. 1997). DMSP operates F15 and F16 satellites in sun-synchronous orbits with nighttime overpasses ranging from about 7 pm to 10 pm local time. The Indian region is observed in two or three OLS orbital passes from each of the satellites, as the swath width is 3,000 km. The OLS is an oscillating scan radiometer with two spectral bands. The visible band pass straddles the visible and near-infrared portion of the spectrum (0.5 to 0.9  $\mu\text{m}$ ) and the thermal band pass covers the 10.5 to 12.5  $\mu\text{m}$  region. At night, the visible band is intensified with a photo-multiplier tube (PMT) to permit detection of clouds illuminated by moonlight. Fire detection using DMSP-OLS nighttime data is based on the identification of lights outside the set of known persistent (stable) lighting sources. Stable lights data-base over Indian region is generated using a time series of OLS data. The basic procedures used to generate the stable lights image have been described elsewhere (Elvidge et al. 1997). Lights found on land, but outside the stable lights mask are possible fires. The initial steps for generating OLS fire product, including the identification of lights and clouds, missing data, and bad scan lines, plus geolocation are fully automated and are described elsewhere (Elvidge et al. 2001). The fire occurrences derived from DMSP-OLS were validated with other sensors data and ground observations (Kiran Chand et al. 2006, 2007; Badarinath et al. 2007a, b, c; Kharol and Badarinath 2006).

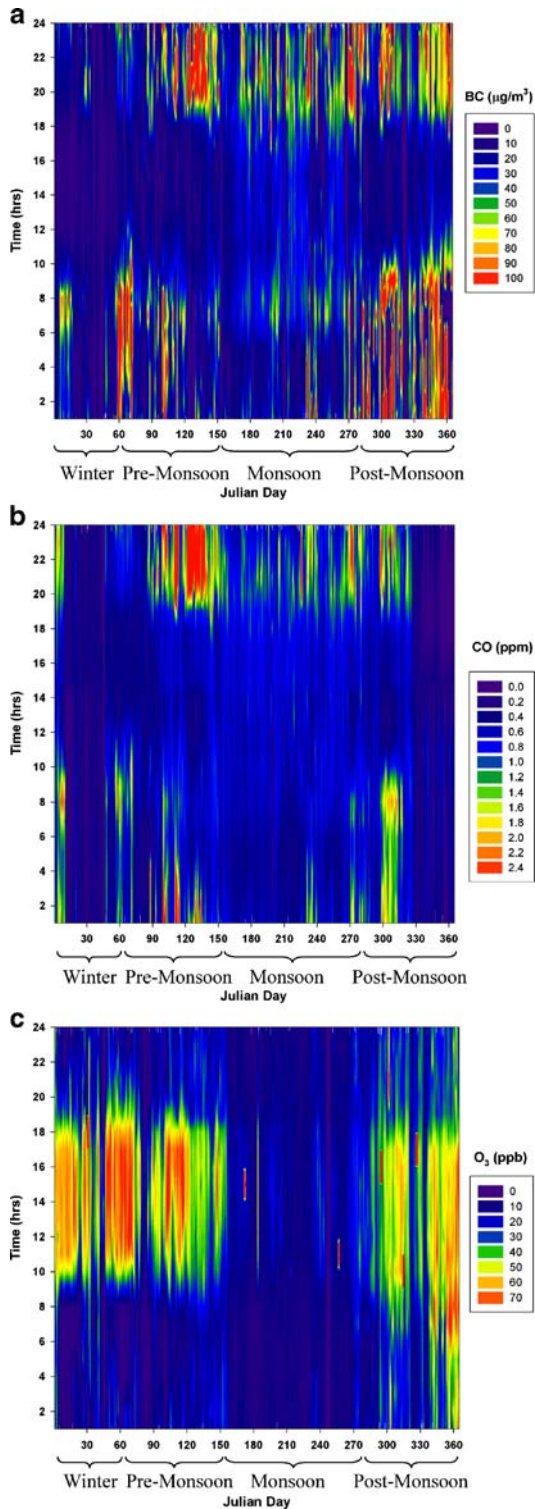
### 2.4 OMI NO<sub>2</sub>

OMI / AURA NO<sub>2</sub> total column and tropospheric column L2 (V00) product from GES-DISC ([http://gdata1.sci.gsfc.nasa.gov/daac-bin/G3/gui.cgi?instance\\_id=omil2g](http://gdata1.sci.gsfc.nasa.gov/daac-bin/G3/gui.cgi?instance_id=omil2g)) at 0.25 deg were used in the study. Atmospheric NO<sub>2</sub> column densities uses the Differential Optical Absorption Spectroscopy (DOAS) technique and are retrieved using spectral measurements of the solar irradiance and earth shine radiance in the wavelength region 415–465 nm using the instrument's VIS detector at a spectral resolution of 0.5 nm (Celarier et al. 2008). Detailed descriptions of the algorithm for the standard OMI NO<sub>2</sub> data product are given elsewhere (Bucsela et al. 2006; Celarier et al. 2008).

## 3 Results and discussion

Figure 1a–c shows the diurnal variation of black carbon (BC) aerosol mass concentration, carbon monoxide (CO) and ozone (O<sub>3</sub>) for the period of January–December, 2008. The urban region of Hyderabad is prone to significant anthropogenic impacts due to increase in population and related factors. The BC mass concentration exhibited diurnal variation with an afternoon minimum and nocturnal maximum, which occurs 2–4 h after the local sunset, subsequently BC mass concentration decreased towards morning and short lived peak occurred shortly after the local sunrise. The observed diurnal variation of BC mass concentration was mainly attributed to the dynamics of the atmospheric boundary layer,

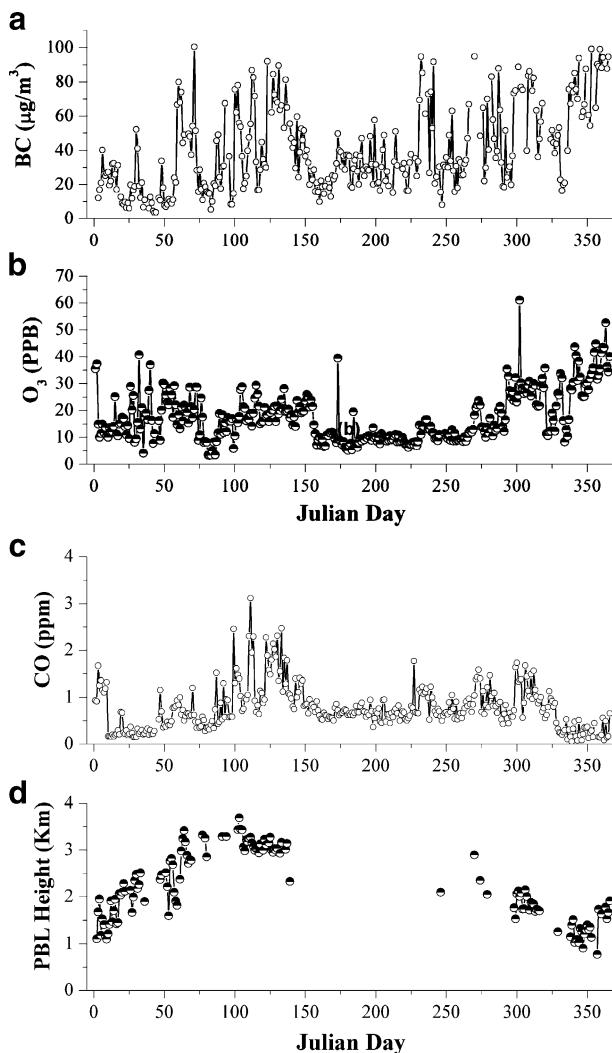
**Fig. 1 a–c** Diurnal variation of black carbon (BC) aerosol mass concentration, carbon monoxide (CO), and ozone ( $O_3$ ) during different seasons, i.e., winter (January–February), pre-monsoon (March–May), monsoon (June–September) and post-monsoon (October–December) during 2008



local vehicular pattern and burning of fossil fuels. The higher values of CO were observed during early morning hours and are strongly related to morning rush-hour vehicular traffic and urbanization effect (Bossioli et al. 2009). Higher concentrations of CO during the late evening hours were attributed to the decreasing height of the mixed layer and stable atmospheric conditions (Latha and Badarinath 2003a, b; Badarinath et al. 2007a, b).

In contrast to CO and BC, ozone gradually increased after sunrise, attaining maximum values during noon and late afternoon, attributed mainly to photo oxidation of precursor gases such as CO, CH<sub>4</sub> and NHMCs in presence of sufficient amount of NO<sub>x</sub> (Fig. 1c). In addition, boundary layer process and meteorological parameters also play a key role in O<sub>3</sub> variability. Higher ozone concentration was observed during pre-monsoon, post-monsoon and winter whereas lowest concentrations exhibited during monsoon season. In pre-monsoon season, maximum ozone concentration are found at measurement site is associated with favourable conditions for high ozone formation. The high temperature,

**Fig. 2 a–d** Julian day variation of nighttime averaged BC, O<sub>3</sub>, CO and PBL height over tropical urban region of Hyderabad, India for the period of January–December, 2008



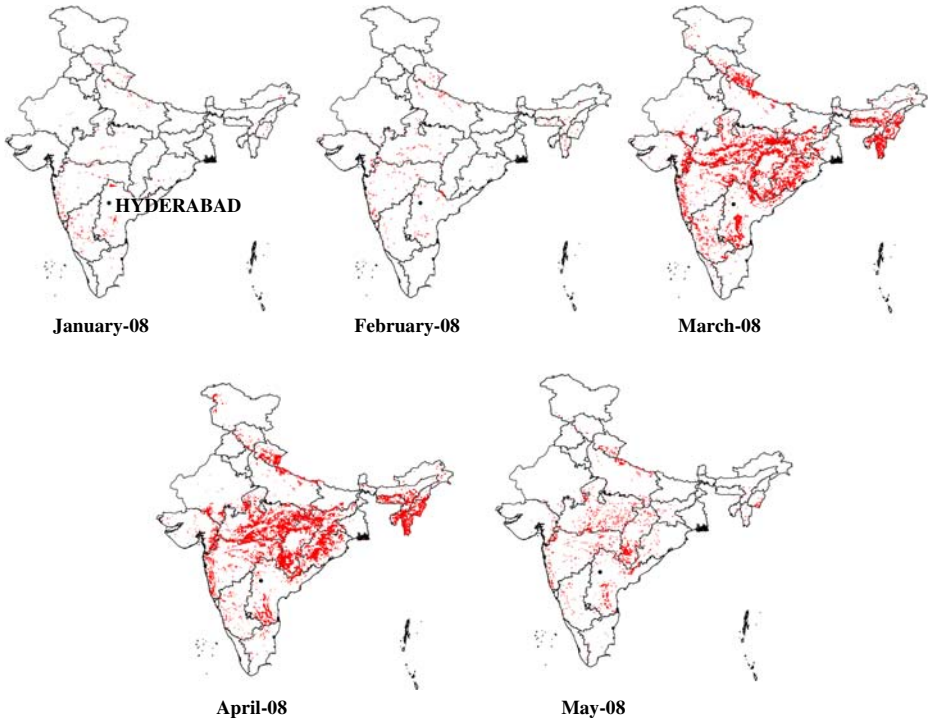
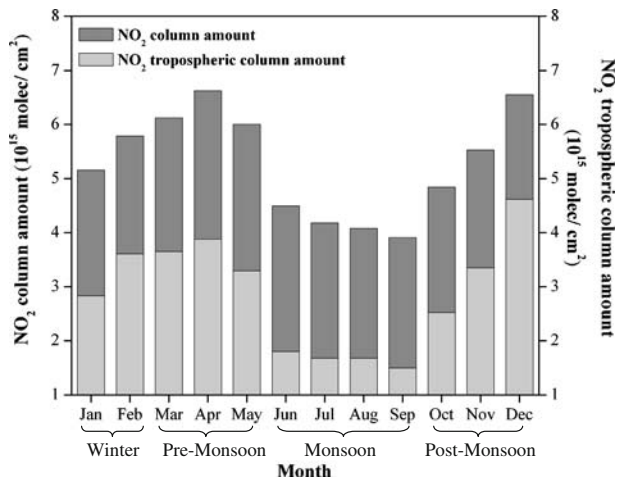


**Fig. 3** DMSP-OLS derived nighttime forest fires over India region during January–May, 2008

high intensity solar radiation and relatively high concentration of NO resulting in the observed ozone maximum in pre-monsoon season. During post-monsoon and winter months ozone concentrations are observed to be high due to higher amounts of precursor gases, in spite of lower solar radiation. Higher levels of precursors during post-monsoon and winter are due to large scale transportation from the continents and lower boundary layer height. Lower concentrations of ozone are found during monsoon season associated

**Fig. 4** Monthly mean variations in Tropospheric and columnar amount of OMI-NO<sub>2</sub> over urban region of Hyderabad during January–December, 2008





with insufficient sun light for photochemical ozone production and scavenging of pollutants by rain. The observed seasonal patterns in ozone concentration over Hyderabad are in agreement with other studies over the region (Reddy et al. 2008).

Figure 2a–d shows the Julian day variation of daily averaged nighttime BC, O<sub>3</sub>, CO and Planetary Boundary Layer height (PBL) for the period of 1st January to 31st December, 2008 at the study site. BC aerosol mass concentration varied between 15 and 100  $\mu\text{g}/\text{m}^3$  during the study period. Higher values of BC on certain Julian days (i.e. 58–61, 69–71, 86–87, 92, 99–103, 109–113, 122–138 and 146–148) are associated with additional loading

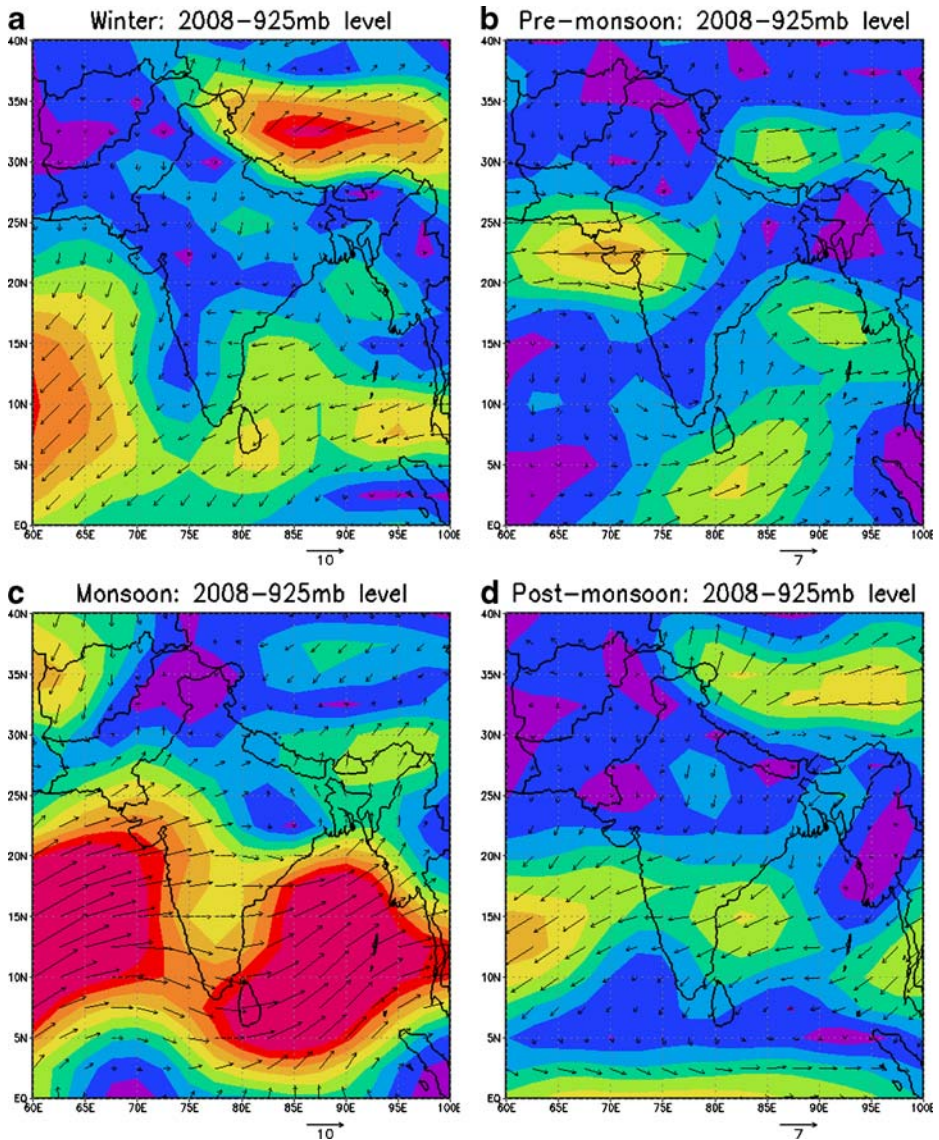


**Fig. 5** NCEP/NCAR reanalysis winds at 925 mb over Indian region during winter, pre-monsoon, monsoon and post-monsoon season



due to forest fire activity over the region during March–May, 2008 (Fig. 3). BC mass concentration showed considerable decrease during monsoon season (June–September) i.e. Julian days from 153 to 274 (Fig. 2a) and mainly attributed to rainfall induced scavenging effect. Earlier study carried out by Latha et al. (2005), suggested a reduction of  $\sim 3.6 \mu\text{g}/\text{m}^3$  in atmospheric black carbon aerosol loading for every 1 mm increase in rainfall intensity over the study site.

Considerable increase in BC mass concentration was observed during post monsoon season (October–December) i.e. Julian days from 275 to 366. The high BC values on certain Julian days during post-monsoon season were mainly attributed to long range transport of anthropogenic emissions from agriculture crop residue burning over the Indo-Gangetic Plains (IGPs). The long-range transport of aerosols/trace gases during forest fire/agriculture crop residue burning season over the region is well described in Kharol and Badarinath (2006); Badarinath et al. (2007a, b); Badarinath et al. (2009a, b). The nighttime mean ozone values exceeded  $\sim 40$  ppb on few days only during the year. Information on PBL and winds are important to understand the transportation and diffusion of pollutants in the boundary layer. The change of mean nocturnal  $\text{O}_3$  values in PBL depends on many factors, such as anthropogenic emissions and atmospheric dispersion conditions (Lal et al. 2000). It is clear from the Fig. 2b that nighttime  $\text{O}_3$  values are lower in second fortnight of March–May months (except certain Julian days) than in February. The changes in nighttime  $\text{O}_3$  values are probably due to different amount and reactivity of  $\text{O}_3$  depletion components such as  $\text{NO}$ ,  $\text{VOC}$ , secondary organic aerosol (SOA) in different environmental and

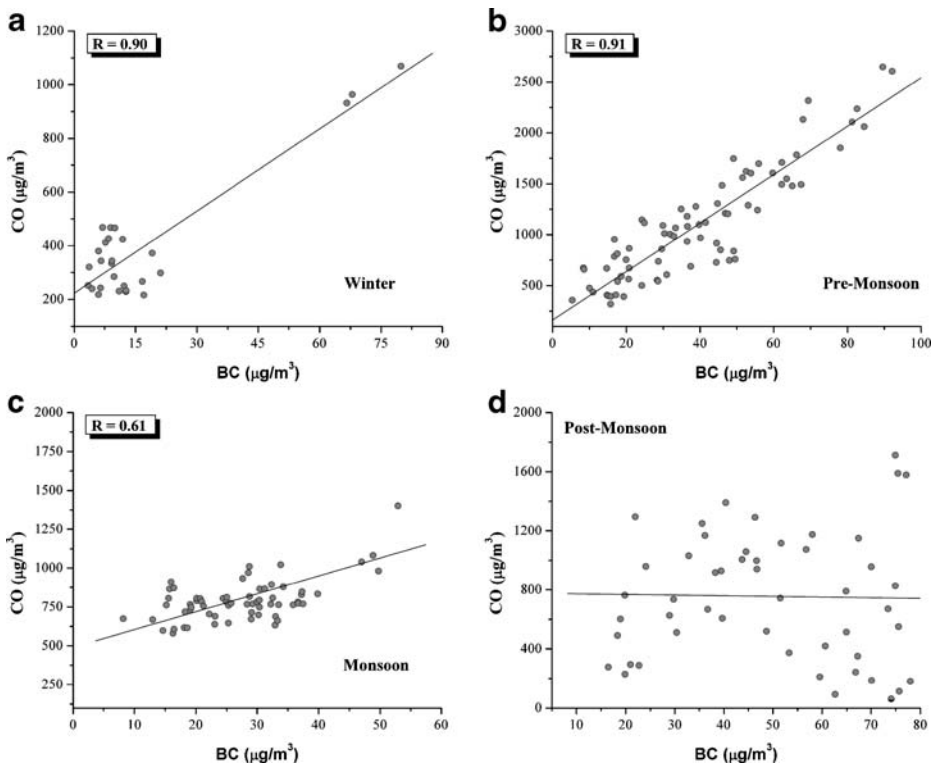


**Fig. 6** a–d Scatter plot between nighttime BC v/s CO during a Winter season b pre-monsoon season c monsoon and d post-monsoon season

meteorological conditions. Nitrogen oxides ( $\text{NO}_x$ ) play a crucial role in the production of ozone via photochemistry. The monthly mean of OMI- $\text{NO}_2$  column and tropospheric column amount shown in Fig. 4 suggested higher values during winter, pre-monsoon and post-monsoon season and have been attributed to biomass burning due to forest fires (shown in Fig. 3) and agriculture crop residue burning over the region. The surface ozone values correlated well with OMI- $\text{NO}_2$  variations. Recent study by Ghude et al. (2008) highlighted major  $\text{NO}_2$  emission hot spots, trends and seasonal cycle over different regions of India and observed emission hot spots over major urban and industrial regions. In addition to higher concentration of BC, CO also showed increasing pattern over the region mainly attributed to anthropogenic emissions due to forest fire activities in pre-monsoon season. It can be seen from Fig. 2c that elevated levels of CO concentrations ranging from 1.5 to 3.4 ppm were observed during March to April, 2008 corresponding to Julian days 87 to 135. Higher concentrations of CO on certain Julian days are due to combinations of anthropogenic emissions, boundary layer processes, chemistry as well as local sources and wind patterns (Latha and Badarinath 2003a, b).

Figure 2d shows the daily averaged nighttime boundary layer height variations obtained from Lidar measurements, for the study period. Boundary layer height varied between 1 to ~3.7 km during January–December-2008 (Fig. 2d). The majority of data showed steady conditions with strong temperature inversions. Shallow boundary layer height during winter

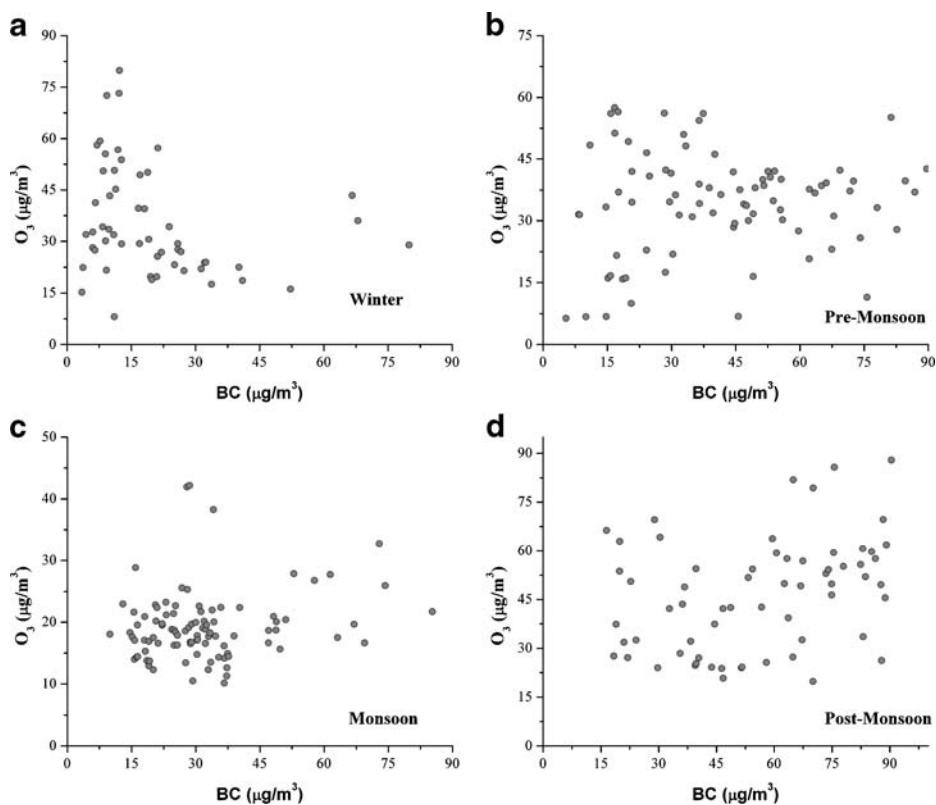


**Fig. 7** a–d Scatter plot between nighttime BC v/s  $\text{O}_3$  during a Winter season b pre-monsoon season c monsoon and d post-monsoon season

(January–February) corresponded with low nighttime temperature. Also, boundary layer height increased during pre-monsoon period (March–May) and coincided with increase in nighttime temperature. During monsoon season (June–September), very few measurements of LIDAR were carried out.

In order to understand the increased loadings of BC and CO during night time, daily nighttime forest fire data derived from DMSP-OLS satellite over the Indian region was analyzed for January–May, 2008. Monthly composites of DMSP-OLS nighttime forest fire locations over Indian region during January–May, 2008 are shown in Fig. 3. Satellite data revealed fire intensity to be high during March–April, 2008. Also, fire counts were relatively higher in states like Andhra Pradesh, Chattisgarh, Orissa, Maharashtra and Madhya Pradesh, which are spatially closer to the measurement site (Fig. 3). Figure 5a–d shows the mean composite vector wind at 925-mb level over the Indian region during winter, pre-monsoon, monsoon and post-monsoon season obtained from NCEP/NCAR reanalysis. The winds over the Indian subcontinent are generally low and exhibit higher speeds over the oceanic areas during winter season. The wind flows mainly from eastern/northeastern directions, carrying significant amounts of pollutants over the region. In general, during premonsoon season (March–May), the weather over Indian region is hot with a daily maximum temperature of around 40°C, and the surface winds are mostly gusty. NCEP winds suggested that air masses advecting from regions having higher fire

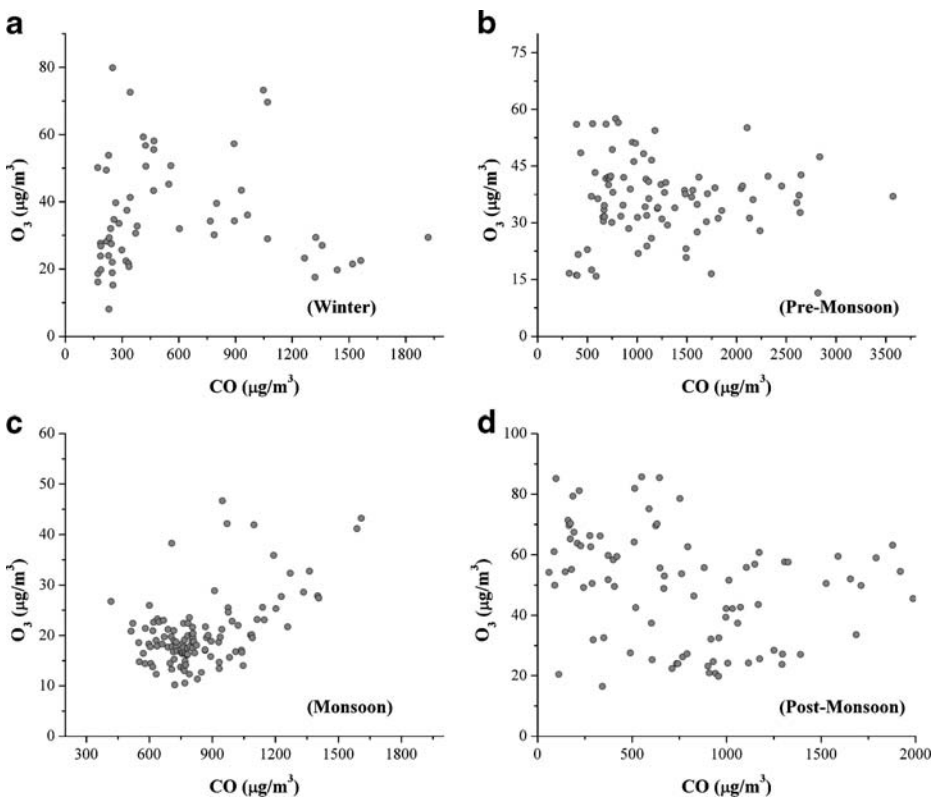


**Fig. 8** a–d Scatter plot between nighttime CO v/s O<sub>3</sub> during a Winter season b pre-monsoon season c monsoon and d post-monsoon season

occurrences during March–May (pre-monsoon season) results in additional loading of aerosols and trace gases over the study area (Fig. 5b). This is also reflected in Fig. 2a–c with nighttime peak in BC, CO and ozone on certain Julian days over the region.

The scatter plot between nighttime average black carbon (BC) aerosol mass concentration and carbon monoxide (CO) showed good correlation ( $R=0.90$ ,  $R=0.91$ ,  $R=0.61$ ) respectively during winter, pre-monsoon and monsoon seasons, however large scatter were observed during post-monsoon season (Fig. 6a–d). However, nighttime averaged tropospheric ozone showed decreasing pattern with increase in BC and CO concentration as shown in Figs. 7a–d and 8a–d. This has been attributed to aggregate structure of soot particles, which offer a large specific surface area for heterogeneous interactions with reactive trace gases like ozone (Badarinath et al. 2007b).

#### 4 Conclusions

In the present study, variations of Ozone, Carbon monoxide and Black Carbon (BC) mass concentration were analyzed in relation to Planetary Boundary Layer height (PBL) from LIDAR measurements and other meteorological conditions during January–December, 2008 in tropical urban area of Hyderabad, India. Results of the study suggested that:

- Higher values of BC and CO observed during early morning hours is attributed to morning rush-hour vehicular traffic whereas  $O_3$  to photooxidation of precursor trace gases.
- Boundary layer height showed positive correlation with increase in night-time ozone concentration.
- The scatter plot between nighttime average black carbon (BC) aerosol mass concentration and carbon monoxide (CO) showed good correlation, suggesting the possibility of similar sources.
- Analysis of DMSP-OLS night time fire data in conjunction with wind vector fields suggested strong correlations of fire events with BC and CO concentrations and possible enhancement during pre-monsoon season through long-range transport, in the study area.

**Acknowledgements** The authors thank the Director of NRSC & Dy. Director (RS&GIS-AA), NRSC for necessary support and facilities. Authors are grateful to ISRO-GBP for financial support. Also authors thank Dr. Chris Elvidge, NGDC, and NOAA, USA for DMSP-OLS night time fire products.

#### References

- Andreae, M.O., Merlet, P.: Emission of trace gases and aerosols from biomass burning, *Global Biogeochem. Cycles* **15**, 955–966 (2001)
- Badarinath, K.V.S., Kiran Chand, T.R., Prasad, V.K.: Agriculture crop residue burning in the Indo-Gangetic plains—a study using IRS P6 AWiFS satellite. *Curr. Sci.* **91**, 1085–1089 (2006)
- Badarinath, K.V.S., Kharol, S.K., Kiran Chand, T.R.: Use of satellite data to study the impact of forest fires over the northeast region of India. *IEEE Geosci. Remote Sens. Lett.* **4**, 485–489 (2007a)
- Badarinath, K.V.S., Kharol, S.K., Kiran Chand, T.R., Parvathi, Y.G., Anasuya, T., Jyothsna, A.N.: Variations in black carbon aerosol, carbon monoxide and ozone over an urban area of Hyderabad, India, during the forest fire season. *Atmos. Res.* **85**, 18–26 (2007b)
- Badarinath, K.V.S., Kharol, S.K., Latha, K.M., Kiran Chand, T.R., Krishna Prasad, V., Nirmala Jyothsna, A., Samatha, K.: Multiyear ground-based and satellite observations of aerosol properties over a tropical urban area in India. *Atmos. Sci. Lett.* **8**, 7–13 (2007c)

- Badarinath, K.V.S., Kharol, S.K., Kaskaoutis, D.G., Kambezidis, H.D.: Case study of dust storm over Hyderabad area, India: its impact on solar radiation using satellite data and ground measurements. *Sci. Total Environ.* **384**, 316–332 (2007d)
- Badarinath, K.V.S., Sharma, A.R., Kharol, S.K.: Impact of emissions from anthropogenic sources on satellite-derived reflectance. *Adv. Space Res.* **43**, 1545–1554 (2009a)
- Badarinath, K.V.S., Kharol, S.K., Sharma, A.R.: Long-range transport of aerosols from agriculture crop residue burning in Indo-Gangetic Plains—a study using LIDAR, ground measurements and satellite data. *J. Atmos. Sol.-Terr. Phys.* **71**(1), 112–120 (2009b)
- Bossioli, E., Tombrou, M., Dandou, A., Athanasopoulou, E., Varotsos, K.V.: The role of planetary boundary layer parameterizations in the air quality of an urban area with complex topography. *Boundary Layer Meteorol.* **131**, 53–72 (2009)
- Bucsel, E.J., Celarier, E.A., Wenig, M.O., Gleason, J.F., Veefkind, J.P., Booersma, K.F., Brinksma, E.J.: Algorithm for NO<sub>2</sub> vertical column retrieval from the ozone monitoring instrument. *IEEE Trans. Geosci. Remote Sens.* **44**(5), 1245–1258 (2006)
- Celarier, E., Brinksma, E., Gleason, J., Wenig, M., Veefkind, J., Cede, A., Herman, J., Ionov, D., Goutail, F., Pommereau, J.-P., Lambert, J.-C., Roozendahl, M., van Pinardi, G., Wittrock, F., Schonhardt, A., Richter, A., Ibrahim, O., Wagner, T., Bojkov, B., Mount, G., Bucsel, E., Swart, D., Volten, H., Kroon, M., Levelt, P.: Validation ozone monitoring instrument nitrogen dioxide columns. *J. Geophys. Res.* **113**, D15S15 (2008). doi:10.1029/2007JD008908
- Chen, W., Kuze, H., Uchiyama, A., Suzuki, Y., Takeuchi, N.: One-year observation of urban mixed layer characteristics at Tsukuba, Japan using a micro pulse lidar. *Atmos. Environ.* **35**, 4273–4280 (2001)
- Collier, C.G., Davies, F., Bozier, K.E., Holt, A.R., Middleton, D.R., Pearson, G.N., Siemen, S., Willetts, D. V., Upton, G.J.G., Young, R.L.: Dual Doppler lidar measurements for improving dispersion models. *Bull. Am. Meteorol. Soc.* **86**, 825–838 (2005)
- Cooke, W.F., Jennings, S.G., Spain, T.G.: Black carbon measurements at Mace Head, 1989–1996. *J. Geophys. Res.* **102**, 25, 339–25,346 (1997)
- Elvidge, C.D., Baugh, K.E., Kihn, E.A., Kroehl, H.W., Davis, E.R.: Mapping of city lights using DMSP operational line scan system data. *Photogramm. Eng. Remote Sensing* **63**, 727–734 (1997)
- Elvidge, C.D., Nelson, I., Hobson, V.R., Safran, J., Baugh, K.E.: Detection of fires at night using DMSP-OLS data. In: Ahern, F.J., Goldammer, J.G., Justice, C.O. (eds.) *Global and Regional Vegetation Fire Monitoring from Space: Planning a Coordinated International Effort*, pp. 125–144. SPB Academic, The Hague (2001)
- Ghude, S.D., Fadnavis, S., Beig, G., Polade, S.D., van der A, R.J.: Detection of surface emission hot spots, trends, and seasonal cycle from satellite-retrieved NO<sub>2</sub> over India. *J. Geophys. Res.* **113**, D20305 (2008). doi:10.1029/2007JD009615
- Goyal, S.K., Ghatge, S.V., Nema, P., Tamhane, S.M.: Understanding urban vehicular pollution problem vis-a-vis ambient air quality—case study of a Megacity (Delhi, India). *Environ. Monit. Assess.* **119**, 557–569 (2006)
- Jain, S., Khare, M.: Urban air quality in mega cities: a case study of Delhi City using vulnerability analysis. *Environ. Monit. Assess.* **136**, 257–265 (2008)
- Kharol, S.K., Badarinath, K.V.S.: Impact of biomass burning on aerosol properties over tropical urban region of Hyderabad, India. *Geophys. Res. Lett.* **33**, L20801 (2006). doi:10.1029/2006GL026759
- Kiran Chand, T.R., Badarinath, K.V.S., Krishna Prasad, V., Murthy, M.S.R., Elvidge, C.D., Tuttle, B.T.: Monitoring forest fires over the Indian region using defense meteorological satellite program-operational linescan system nighttime satellite data. *Remote Sens. Environ.* **103**(2), 165–178 (2006)
- Kiran Chand, T.R., Badarinath, K.V.S., Murthy, M.S.R., Rajshekhar, G., Elvidge, C.D., Tuttle, B.T.: Active forest fire monitoring in Uttaranchal State, India using multi-temporal DMSP-OLS and MODIS data. *Int. J. Remote Sens.* **28**(10), 2123–2132 (2007)
- Klett, J.D.: Stable analytical inversion solution for processing lidar returns. *Appl. Opt.* **20**(211), 220 (1981)
- Kumar, Y.B.: Portable lidar system for atmospheric boundary layer measurements. *Opt. Eng.* **45**, 076201 (2006)
- Lal, S., Naja, M., Subbaraya, B.H.: Seasonal variations in surface ozone and its precursors over an urban site in India. *Atmos. Envi.* **34**(17), 2713–2724 (2000)
- Latha, K.M., Badarinath, K.V.S.: Black carbon aerosols over tropical urban environment—a case study. *Atmos. Res.* **69**, 125–133 (2003a)
- Latha, K.M., Badarinath, K.V.S.: Diurnal and seasonal variations of NO<sub>x</sub> over urban environment—a case study from Hyderabad. *India. Indian J. Environ. Sci.* **7**, 63–73 (2003b)
- Latha, K.M., Badarinath, K.V.S., Reddy, P.M.: Scavenging efficiency of rainfall on black carbon aerosols over an urban environment. *Atmos. Sci. Lett.* **6**(3), 148–151 (2005)
- Logan, J.A., Prather, M.J., Wofsy, S.C., McElroy, M.B.: Tropospheric chemistry: a global perspective. *J. Geophys. Res.* **86**, 7210–7254 (1981)



- Molina, M.J., Molina, L.T.: Megacities and atmospheric pollution. *J. Air Waste Manage. Assoc.* **54**(6), 644–680 (2004)
- Nair, P.R., Chand, D., Lal, S., Modh, K.S., Naja, M., Parameswaran, K., Ravindran, S., Venkataramani, S.: Temporal variations in surface ozone at Thumba (8.6° N, 77° E) a tropical coastal site in India. *Atmos. Environ.* **36**, 603–610 (2002)
- Naja, M., Lal, S.: Surface ozone and precursor gases at Gadanki (13.5° N, 79.2° E), a tropical rural site in India. *J. Geophys. Res.* **107**(D14), 4197 (2002). doi:[10.1029/2001JD000357](https://doi.org/10.1029/2001JD000357)
- Reddy, R.R., Ram Gopal, K., Narasimhulu, K., Reddy, L.S.S., Kumar, K.R., Ahammed, N., Rao, T.V.R., Abdul Azeem, P.: Diurnal and seasonal variabilities in surface ozone and its precursor gases at semi-arid site Anantapur (14.62° N, 77.65° E, 331 m asl) in India. *Int. J. Environ. Stud.* **65**(2), 247–265 (2008)